J|A|C|S
ARTICLES
Published on Web 05/06/2006

Unidirectional Electronic Ring Current Driven by a Few Cycle Circularly Polarized Laser Pulse: Quantum Model Simulations for Mg−Porphyrin

Ingo Barth, Jörn Manz,* Yasuteru Shigeta, and Kiyoshi Yagi

Contribution from the Institut für Chemie und Biochemie, Freie Universität Berlin, Takustr. 3, 14195 Berlin, Germany, and Department of Applied Chemistry, School of Engineering, The University of Tokyo, 7-3-1 Hongo, Bunkyo, Tokyo 113-8656, Japan

Received October 21, 2005; E-mail: jmanz@chemie.fu-berlin.de

Abstract: A circularly polarized ultraviolet (UV) laser pulse may excite a unidirectional valence-type electronic ring current in an oriented molecule, within the pulse duration of a few femtoseconds (e.g., $\tau = 3.5$ fs). The mechanism is demonstrated by quantum model simulation for $|X\rangle = |1\ ^1A_{1g}\rangle \rightarrow |E_+\rangle = |4\ ^1E_{u+}\rangle$ population transfer in the model system, Mg−porphyrin. The net ring current generated by the laser pulse ($I = 84.5$ μA) is at least 100 times stronger than any ring current, which could be induced by means of permanent magnetic fields, with present technology.

1. Introduction

The purpose of this paper is to suggest a new mechanism for the induction of selective electronic ring currents in molecules: excitation by a few cycle circularly polarized UV laser pulse, within a few femtoseconds (fs). It is motivated by recent advances in laser technology which provide the tools for the present approach, from circularly polarized pulses with controlled shape in the fs[1] toward the attosecond (as) time domain (see also refs 2−4). It may be considered *cum grano salis* as ultrashort, molecular scale analogy of previous preparations of electronic Rydberg atom wave packets which circulate along classical Kepler paths with diameters of several thousands of bohr radii (a_0) on the microsecond (ms) time scale, driven by circularly polarized nanosecond (ns) to few hundreds of picoseconds (ps) laser pulses combined with radio frequency fields; see the pioneering work by Yeazell and Stroud, Jr.[5,6] Stimulating extensions to laser control of Rydberg wave packets have been demonstrated in refs 7−10. Another important analogy is selective electron transfer induced by linearly polarized laser pulses in the fs time domain, as suggested recently by Krause et al.[11] Moreover, our approach is complementary to traditional generation of electronic ring currents by magnetic fields (see, for example, refs 12−16). Last, but not least, it is also motivated by previous demonstrations of unidirectional nuclear torsional motions induced by means of circularly polarized IR π laser pulses, specifically for preparing pure enantiomers from an oriented racemate[17] or for driving molecular rotors,[18] compared with alternative approaches based on linearly polarized pulses.[19−21] By analogy, ultrashort circularly polarized UV laser pulses should also be efficient tools for circulating electrons. In general, it is well-known that the helicity of circularly polarized laser pulses may be transferred to matter by combined electric plus magnetic dipole couplings; see, for example, the simulations for enantiomeric excesses obtained from racemic mixtures by applying circularly polarized pulsed lasers to a randomly oriented model two-level chiral molecule,[22] but it remains a challenge whether the laser pulses will drive the electrons selectively, or the nuclei, or both.

Our approach will be demonstrated by quantum simulations for the model system, magnesium−porphyrin, based on previous electronic structure ab initio calculations by Rubio et al.[23] and by Sundholm[24] (see also refs 25 and 26). For this purpose, we assume that the system has been preoriented in the laboratory-fixed *x*/*y*-plane, as indicated in Figure 1, for example, by the

(1) Brixner, T.; Gerber, G. *Opt. Lett.* **2001**, *16*, 557.
(2) Hentschel, M.; Kienberger, R.; Spielmann, Ch.; Reider, G. A.; Milosevic, N.; Brabec, T.; Corkum, P.; Heinzmann, U.; Drescher, M.; Krausz, F. *Nature* **2001**, *414*, 509.
(3) Strelkov, V.; Zaïr, A.; Tcherbakoff, O.; López-Martens, R.; Cormier, E.; Mével, E.; Constant, E. *Appl. Phys. B* **2004**, *78*, 879.
(4) Kitzler, M.; O'Keefee, K.; Lezius, M. *J. Mod. Opt.* **2005**, *53*, 57.
(5) Yeazell, J. A.; Stroud, C. R., Jr. *Phys. Rev. A* **1987**, *35*, 2806.
(6) Yeazell, J. A.; Stroud, C. R., Jr. *Phys. Rev. Lett.* **1988**, *60*, 1494.
(7) Noordam, L. D.; Jones, R. R. *J. Mod. Opt.* **1997**, *44*, 2515.
(8) Weinacht, T. C.; Ahn, J.; Bucksbaum, P. H. *Phys. Rev. Lett.* **1998**, *80*, 5508.
(9) Weinacht, T. C.; Ahn, J.; Bucksbaum, P. H. *Nature* **1999**, *397*, 233.
(10) Maeda, H.; Norum, D. V. L.; Gallagher, T. F. *Science* **2005**, *307*, 1757.
(11) Krause, P.; Klamroth, T.; Saalfrank, P. *J. Chem. Phys.* **2005**, *123*, 074105.
(12) Lazzeretti, P. *Prog. Nucl. Magn. Reson. Spectrosc.* **2000**, *36*, 1.
(13) Steiner, E.; Fowler, P. W. *J. Phys. Chem. A* **2001**, *105*, 9553.
(14) Steiner, E.; Soncini, A.; Fowler, P. W. *Org. Biomol. Chem.* **2005**, *3*, 4053.
(15) Heine, T.; Corminboeuf, C.; Seifert, G. *Chem. Rev.* **2005**, *105*, 3889.
(16) Jusélius, J.; Sundholm, D. *J. Org. Chem.* **2000**, *65*, 5233.
(17) Hoki, K.; Kröner, D.; Manz, J. *Chem. Phys.* **2001**, *267*, 59.
(18) Hoki, K.; Yamaki, M.; Koseki, S.; Fujimura, Y. *J. Chem. Phys.* **2003**, *118*, 497.
(19) Shapiro, M.; Frishman, E.; Brumer, P. *Phys. Rev. Lett.* **2000**, *84*, 1669.
(20) Fujimura, Y.; González, L.; Hoki, K.; Kröner, D.; Manz, J.; Ohtsuki, Y. *Angew. Chem., Int. Ed.* **2000**, *39*, 4586.
(21) Fujimura, Y.; González, L.; Kröner, D.; Manz, J.; Mehdaoui, I.; Schmidt, B. *Chem. Phys. Lett.* **2004**, *386*, 248.
(22) Salam, A.; Meath, W. J. *Chem. Phys.* **1998**, *228*, 115.
(23) Rubio, M.; Roos, B. O.; Serrano-Andrés, L.; Merchán, M. *J. Chem. Phys.* **1999**, *110*, 7202.
(24) Sundholm, D. *Chem. Phys. Lett.* **2000**, *317*, 392.
(25) Hasegawa, J.; Hada, M.; Nonoguchi, M.; Nakatsuji, N. *Chem. Phys. Lett.* **1996**, *250*, 159.
(26) Baerends, E. J.; Ricciardi, G.; Rosa, A.; van Gisbergen, S. J. A. *Coord. Chem. Rev.* **2002**, *230*, 5.

10.1021/ja057197l CCC: $33.50

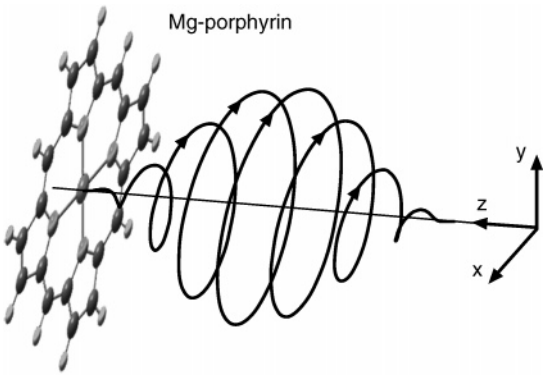

Figure 1. Eight-cycle right circularly polarized laser pulse propagating along the *z*-direction in order to induce the unidirectional right ring current in Mg−porphyrin, preoriented in the *x*/*y*-plane (schematic, cf. ref 28). The arrows indicate the time evolution of the electric field acting on the molecule, which appears clockwise ("right") when viewed along the *z*-direction of propagation.

methods of ref 27. The model and techniques are specified in section 2, and the results and conclusions are in sections 3 and 4, respectively.

2. Model and Techniques

The electron dynamics of Mg−porphyrin oriented in the *x*/*y*-plane and driven by a few cycle circularly polarized laser pulse propagating along the *z*-direction (see Figure 1) is described in semiclassical dipole approximation, by means of the time-dependent electronic Schrödinger equation

$$i\hbar|\dot{\Psi}(t)\rangle = (H_{\mathrm{el}} - \underline{M}\cdot\underline{\varepsilon}_{\pm}(t))|\Psi(t)\rangle \tag{1}$$

with electronic Hamilton operator

$$H_{\mathrm{el}} = -\frac{\hbar^2}{2m_{\mathrm{e}}}\sum_{i=1}^{N}\nabla_i^2 + \frac{e^2}{4\pi\epsilon_0}\left(\sum_{\substack{\alpha,\beta=1\\ \beta>\alpha}}^{N'}\frac{Z_\alpha Z_\beta}{|\underline{R}_\alpha - \underline{R}_\beta|} - \sum_{i=1}^{N}\sum_{\alpha=1}^{N'}\frac{Z_\alpha}{|\underline{r}_i - \underline{R}_\alpha|} + \sum_{\substack{i,j=1\\ j>1}}^{N}\frac{1}{|\underline{r}_i - \underline{r}_j|}\right) \tag{2}$$

and dipole operator

$$\underline{M} = -e\sum_{i=1}^{N}\underline{r}_i + e\sum_{\alpha=1}^{N'}Z_\alpha\underline{R}_\alpha \tag{3}$$

In eqs 2 and 3, the symbols have their usual meanings, that is $\underline{r}_i$ and $\underline{R}_\alpha$ denote the positions of N electrons and of N' nuclei with charges Z_α, respectively. The right (+) or left (−) circularly polarized laser pulses are specified by

$$\underline{\varepsilon}_{\pm}(t) = \varepsilon_0 s(t)(\cos(\omega t + \eta)\underline{e}_x \pm \sin(\omega t + \eta)\underline{e}_y) \tag{4}$$

with field amplitude ε_0, carrier frequency ω, phase η, and unit vectors $\underline{e}_x$ and $\underline{e}_y$ along the *x*- and *y*-axes. Note that there are two different definitions of right/left circular polarizations of laser pulses in the literature. The present one (eq 4) is according to the handedness convention, also called the angular momentum convention; it is convenient for the subsequent discussion of angular momentum transfer, that is, the *z*-component of the angular momentum of a photon of the right circularly polarized pulse is $+1\ \hbar$, and the resulting electronic current is clockwise when viewed along the direction of propagation.[28] In contrast, the present "right" circularly polarized pulses would be called "left" circularly polarized if one adapts the optics "screw" convention.[29,30] The shape function is chosen (cf. refs 17 and 31) as

$$s(t) = \sin^2\left(\frac{\pi t}{t_{\mathrm{p}}}\right) \tag{5}$$

where t_{p} denotes the total duration of the laser pulse. The full width at half-maximum for the corresponding intensity $I(t) = c\epsilon_0|\underline{\varepsilon}_{\pm}(t)|^2 = c\epsilon_0\varepsilon_0^2 s(t)^2$ is $\tau = ((2/\pi)\ \arccos(1/\sqrt[4]{2}))t_{\mathrm{p}} \approx 0.364t_{\mathrm{p}}$, related to the spectral width Γ according to $\Gamma\tau \approx 3.295\ \hbar$. Below we consider laser pulses with $\tau \approx 3.5$ fs, $\Gamma \approx 0.62$ eV, so that the nuclei may be assumed to be frozen in their equilibrium positions during the laser pulse. Moreover, we consider laser pulses with maximum intensities, $I_{\max} = c\epsilon_0\varepsilon_0^2$, well below 10^{13} Wcm^{-2}, implying negligible ionization. For example, for the subsequent application where $I_{\max} = 1.28 \times 10^{12}$ Wcm^{-2} and using the ionization potential of Mg−porphyrin, $IP = 6.9$ eV,[32] one can estimate the upper limit 1.14×10^{-5} s^{-1} of the ionization rate, based on the tunneling ionization model[33] derived from direct current tunneling theory,[34] as suggested in ref 35—this is indeed entirely negligible, on the time scale of the laser pulse duration. The solution of eq 1 may then be written as

$$|\Psi(t)\rangle = \sum_i C_i(t)|\Psi_i\rangle e^{-iE_i t/\hbar} \tag{6}$$

where E_i denotes the electronic eigenenergies of the electronic states $|\Psi_i\rangle$

$$H_{\mathrm{el}}|\Psi_i\rangle = E_i|\Psi_i\rangle \tag{7}$$

Inserting the ansatz (eq 6) into the time-dependent electronic Schrödinger eq 1 yields the equivalent set of equations for the time-dependent coefficients

$$i\hbar\dot{C}_j(t) = -\underline{\varepsilon}_{\pm}(t)\sum_i C_i(t)\langle\Psi_j|\underline{M}|\Psi_i\rangle e^{-i\tilde{\omega}_{ij}t} \tag{8}$$

with transition frequencies

$$\tilde{\omega}_{ij} = (E_i - E_j)/\hbar \tag{9}$$

In the subsequent application, the molecule is initially in the electronic ground state $|0\rangle = |X\rangle$, that is, $C_i(t=0) = \delta_{0i}$, and the laser frequency ω is tuned resonant to a particular transition frequency, specifically for excitation from $|X\rangle$ to a pair of degenerate excited states with *E*-symmetry, $|i\rangle = |E_+\rangle$ or $|i+1\rangle = |E_-\rangle$, denoted for simplicity as $\tilde{\omega} = \tilde{\omega}_{i0} = \tilde{\omega}_{(i+1)0} = (E_{\mathrm{E}_\pm} - E_X)/\hbar$. Here the complex wave functions, $|E_+\rangle$ and $|E_-\rangle$, may be expressed in terms of two real ones

$$|E_\pm\rangle = \frac{1}{\sqrt{2}}(|E_x\rangle \pm i|E_y\rangle) \tag{10}$$

similar to the relations of complex atomic orbitals $|2p_+\rangle$ and $|2p_-\rangle$ and real ones $|2p_x\rangle$ and $|2p_y\rangle$, or to the degenerate complex toroidal orbitals $|\pi_+\rangle$ and $|\pi_-\rangle$, which carry handedness in diatomic molecules for presentations of clockwise or anticlockwise toroidal electronic currents around the molecular axis, with analogous expressions in terms of the

(27) Stapelfeldt, H.; Seideman, T. *Rev. Mod. Phys.* **2003**, *75*, 543.
(28) IEEE Standart Definitions of Terms for Antennas, IEEE Stand. 145-1983, IEEE Trans. antennas propagat. AP-31, pt II, p 5, 1983, revised IEEE Stand. 145, 1983.
(29) Born, M.; Wolf, B. *Principles of optics: Electromagnetic theory of propagation, interference and diffraction of light*, 7th ed.; Cambridge University Press: Cambridge, 1999.
(30) Shurcliff, W. A. *Polarized light: Production and use*; Harvard University Press: Cambridge, MA, 1962.
(31) Paramonov, G. K.; Savva, V. A. *Phys. Lett. A* **1983**, *97*, 340.
(32) Dolgounitcheva, O.; Zakrzewski, V. G.; Oritz, J. V. *J. Phys. Chem. A* **2005**, *109*, 11596.
(33) Corkum, P. B.; Burnett, N. H.; Brunel, F. *Phys. Rev. Lett.* **1989**, *62*, 1259.
(34) Landau, L. D.; Lifshitz E. M. *Quantum mechanics*; Pergamon: New York, 1965; p 276.

real orbitals $|\pi_x\rangle$ and $|\pi_y\rangle$.[36] The pulse duration, t_p, is chosen such that the corresponding spectral half-width $\Gamma/2$ is smaller than the energy gap between the target level and neighboring states with *E*-symmetry. In analogy to the results of ref 11 for state selective electron transfer driven by linearly polarized laser pulses, the general solution (eq 6) then reduces to approximately three dominant contributions, including the electronic ground and two resonant degenerate excited states of the target level

$$|\Psi(t)\rangle = C_X(t)|X\rangle e^{-iE_X t/\hbar} + C_{E_+}(t)|E_+\rangle e^{-iE_{E+}t/\hbar} + C_{E_-}(t)|E_-\rangle e^{-iE_{E-}t/\hbar} \quad (11)$$

Equation 8 for the time-dependent coefficients may then be rewritten in matrix form as

$$i\hbar \begin{pmatrix} \dot{C}_X(t) \\ \dot{C}_{E_+}(t) \\ \dot{C}_{E_-}(t) \end{pmatrix} = -\underline{\varepsilon}_{\pm}(t) \begin{pmatrix} 0 & \langle X|\underline{M}|E_+\rangle e^{-i\tilde{\omega}t} & \langle X|\underline{M}|E_-\rangle e^{-i\tilde{\omega}t} \\ \langle E_+|\underline{M}|X\rangle e^{i\tilde{\omega}t} & 0 & 0 \\ \langle E_-|\underline{M}|X\rangle e^{i\tilde{\omega}t} & 0 & 0 \end{pmatrix} \begin{pmatrix} C_X(t) \\ C_{E_+}(t) \\ C_{E_-}(t) \end{pmatrix} \quad (12)$$

where we have used the fact that all dipole functions for the electronic ground and excited states as well as the dipole transition elements between the degenerate states $|E_+\rangle$ and $|E_-\rangle$ vanish, due to symmetry. Inserting the right circularly polarized laser field (eq 4) with resonant frequency $\omega = \tilde{\omega}$ yields the simplified set of equations

$$i\hbar \begin{pmatrix} \dot{C}_X(t) \\ \dot{C}_{E_+}(t) \\ \dot{C}_{E_-}(t) \end{pmatrix} = -M\varepsilon_0 s(t) \begin{pmatrix} 0 & 1 & e^{-2i\tilde{\omega}t} \\ 1 & 0 & 0 \\ e^{2i\tilde{\omega}t} & 0 & 0 \end{pmatrix} \begin{pmatrix} C_X(t) \\ C_{E_+}(t) \\ C_{E_-}(t) \end{pmatrix} \quad (13)$$

where M denotes the transition dipole matrix element

$$M = \frac{1}{\sqrt{2}}\langle E_x|M_x|X\rangle = \frac{1}{\sqrt{2}}\langle E_y|M_y|X\rangle \quad (14)$$

Numerical solutions of eq 8 for the time-dependent coefficients $C_i(t)$ with resonant frequency $\omega = \tilde{\omega}$, starting from $C_i(t = 0) = \delta_{0i}$, are calculated by means of Runge−Kutta propagation. The accurate results turn out to be close to the solutions of eq 13 obtained by means of the rotating wave approximation (RWA), that is, neglecting the rapidly oscillating terms $e^{\pm 2i\tilde{\omega}t}$ (cf. refs 22, and 37−39). These RWA solutions yield analytical expressions which are useful for the subsequent discussions. Specifically, on resonance, we obtain

$$C_X(t) = \cos\left(\frac{M\varepsilon_0}{\hbar}\int_0^t s(t')\mathrm{d}t'\right) \quad (15)$$

$$C_{E_+}(t) = i\sin\left(\frac{M\varepsilon_0}{\hbar}\int_0^t s(t')\mathrm{d}t'\right) \quad (16)$$

$$C_{E_-}(t) = 0 \quad (17)$$

that is, the right circularly polarized laser pulse transfers population selectively from $|X\rangle$ to $|E_+\rangle$ excluding the decoupled state $|E_-\rangle$. Inserting the shape function (eq 5) then yields complete population transfer, $C_X(t) = 0$ at $t = t_p$, if

$$|M\varepsilon_0 t_p| = \pi\hbar \quad (18)$$

To prevent the excited state from returning to the ground state, the resulting duration t_p of the π pulse is thus twice as long as the period t_R of Rabi cycling in the case of resonant continuous wave excitation (i.e., $s(t) = 1$ in eqs 15 and 16, yielding $C_X(t_R) = 0$ if $|M\varepsilon_0 t_R| = \pi\hbar/2$).[37] Expressions 4 and 5 together with the condition 18 may be considered as definition of a (right) circularly polarized π laser pulse designed for the target $|X\rangle \rightarrow |E_+\rangle$ transition. The exact solutions of eq 8 yield also small populations $P_i(t) = |C_i(t)|^2$ in neighboring states $|n^1E_{u+}\rangle$ with the same symmetry as the target state. Equivalent expressions are obtained for the corresponding left circularly polarized π laser pulse yielding selective population transfer from $|X\rangle$ to $|E_-\rangle$.

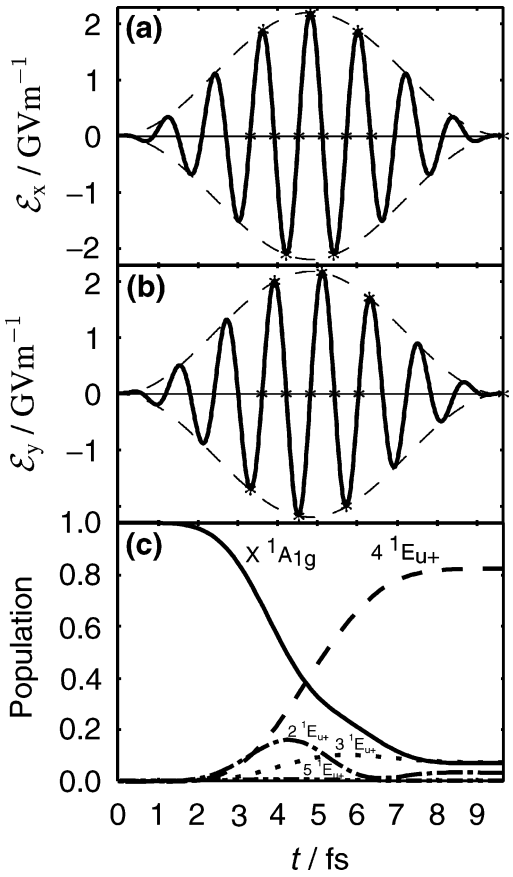

Figure 2. Eight-cycle right circularly polarized UV π laser pulse (eqs 4, 5, and 18) designed for the target $|X\rangle = |1\ ^1A_{1g}\rangle \rightarrow |4\ ^1E_{u+}\rangle$ transition of oriented Mg−porphyrin. Panels a, b, and c show the *x*- and *y*-components of the electric field, and the resulting population transfer from the ground state $|X\rangle$ to the target state $|4\ ^1E_{u+}\rangle$ and neighboring states with the same symmetry $|n\ ^1E_{u+}\rangle$. Symbols ∗ mark the times when the resulting laser driven electron circulation will be illustrated in Figure 3. A perspective view of the laser pulse exciting Mg−porphyrin is shown in Figure 1. The molecular and laser parameters are specified in the text.

3. Results and Discussion

The general approach of section 2 will now be applied to induction of an electronic ring current in oriented Mg−porphyrin, which has D_{4h} symmetry (see Figure 1), driven by an eight-cycle right circularly polarized UV π laser pulse with resonance frequency tuned to the $|X\rangle = |1\ ^1A_{1g}\rangle \rightarrow |4\ ^1E_{u+}\rangle$ transition. The corresponding molecular parameters for states $|X\rangle$, $|n\ ^1E_{u+}\rangle$, $n = 1, 2, 3, 4$ and 5, 6, are adapted from quantum chemical CASPT2(14/16) and TD-DFT calculations by Rubio

(35) Bandrauk, A. D.; Sedlik, E. S.; Matta, C. F. *J. Chem. Phys.* **2004**, *121*, 7764.
(36) Levine, I. N. *Quantum chemistry*; Prentice Hall: New Jersey, 2000.
(37) Sargent, M., III; Scully, M. O.; Lamb, W. E., Jr. *Laser Physics*; Addison-Wesley: London, 1974.
(38) Allen, L.; Eberly, J. H. *Optical resonance and two-level atoms*; Wiley: New York, 1975.
(39) Thomas, G. F. *Phys. Rev. A* **1983**, *27*, 2744.

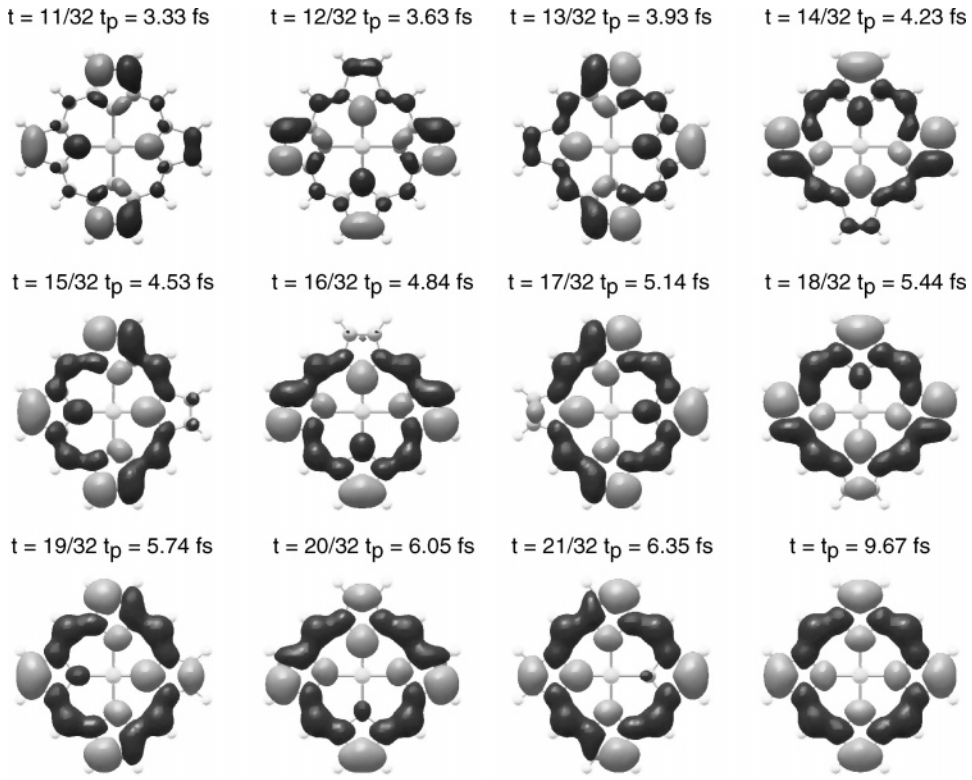

Figure 3. Electron circulation in oriented Mg−porphyrin driven by the circularly polarized UV π laser pulse which propagates along the *z*-axis toward the observer (cf. Figures 1 and 2). The snapshots show the difference between the total electron density at time t and the initial electron density, $\Delta\rho(t) = \rho(t) - \rho(0)$, $\Delta\rho(t) > 0$ (dark area) and $\Delta\rho(t) < 0$ (light area), evaluated for the dominant electronic configurations which contribute to the laser driven $|1\ ^1A_{1g}\rangle \rightarrow |4\ ^1E_{u+}\rangle$ population transfer; see text. The times for the snapshots are between $t = (t_p - \tau)/2 = 3.08$ fs and $t = (t_p + \tau)/2 = 6.60$ fs, as well as $t = t_p = 9.67$ fs. They are also marked by symbols $*$ in Figure 2.

et al.[23] and by Sundholm,[24] respectively, and converted into the corresponding laser parameters, that is, $\hbar\omega = 3.42$ eV and $M = -1.84\ ea_0$. The corresponding time of a laser cycle is $t_c = 2\pi/\omega = 1.21$ fs, the total pulse duration is chosen as $t_p = 8t_c = 9.67$ fs, implying the full width at half-maximum for the intensity $\tau = 3.52$ fs and spectral width $\Gamma = 0.62$ eV, field amplitude $\varepsilon_0 = 2.20 \times 10^9$ Vm^{-1}, and maximum intensity $I_{max} = 1.28 \times 10^{12}$ Wcm^{-2}. The *x*- and *y*-components of the circularly polarized π laser pulse are shown in Figure 2, together with the resulting populations of the initial state, $P_X(t) = |C_X(t)|^2$, the target state $P_{4^1E_{u+}}(t) = |C_{4^1E_{u+}}(t)|^2$, and neighboring states with same symmetry, $P_{n^1E_{u+}}(t) = |C_{n^1E_{u+}}(t)|^2$.

Details of the laser driven electron dynamics may be investigated conveniently in terms of the time evolutions of the dominant electronic configurations which contribute to the population transfer. The initial ground state $|1\ ^1A_{1g}\rangle$ consists of the main contribution, ... $(4a_{2u})^2(1a_{1u})^2$ (weight 80%), whereas the excited target state $|4\ ^1E_{u+}\rangle$ is dominated by $(3a_{2u}) \rightarrow (4e_{g+})$ (weight 57%);[23] see also refs 24−26. For the present analysis, the relevant orbitals, $(3a_{2u})$ and $(4e_{g+})$, were calculated at the HF/6-31G(d) level. The time evolution of the difference between the corresponding total electron density at time t and the initial electron density, $\Delta\rho(t) = \rho(t) - \rho(0)$, is illustrated by means of snapshots in Figure 3. As one sees, $\Delta\rho(t)$ changes from the initial value ($\Delta\rho(0) = 0$) most rapidly during a rather short time interval when the laser intensity is close to its maximum value, from $(t_p - \tau)/2 = 3.08$ fs to $(t_p + \tau)/2 = 6.60$ fs. The snapshots show that the chirality of the laser pulse (see Figures 1 and 2) is converted into corresponding unidirectional (right) intramolecular electron circulation in the oriented Mg−porphyrin, at the same frequency ω as the laser pulse. During the intense domain of the laser pulse, these electron circulations appear to be rather complex, for example, with "whirlpools" in the four equivalent pyrrole fragments. Finally, for $t \rightarrow t_p$, the π laser pulse prepares the electronic eigenstate $|4\ ^1E_{u+}\rangle$, and the electronic density approaches the associated stationary limit, with rather simple structure corresponding to state-selective population transfer (see Figure 3). This target electronic eigenstate $|4\ ^1E_{u+}\rangle$ represents the desired valence-type electronic ring current which is illustrated by means of electronic flux maps in Figure 4.

The time-dependent electronic current density $\underline{j}(\underline{r}, t)$ is given by

$$\underline{j}(\underline{r}, t) = \frac{i\hbar}{2m_e} N \int\cdots\int (\Psi(t)\underline{\nabla}\Psi^*(t) - \Psi^*(t)\underline{\nabla}\Psi(t))\, d\underline{r}_2 ... d\underline{r}_N d\sigma_1 ... d\sigma_N \quad (19)$$

where $\int\cdots\int$ indicates integration over the other $N - 1$ space and all spin variables of N electrons. The dominant contribution to $\underline{j}(\underline{r}, t)$ for $t \geq t_p$ is due to the target state, $|\Psi(t)\rangle \approx |4\ ^1E_{u+}\rangle \exp(-iE_{4^1E_u}t/\hbar + i\tilde{\eta})$ (with irrelevant phase $\tilde{\eta}$) which is characterized by the singly occupied excited orbital $(4e_{g+})$, thus

$$\underline{j}(\underline{r}) \approx \underline{j}_{E_+}(\underline{r}) \approx \underline{j}_{4e_{g+}}(\underline{r}) = \frac{i\hbar}{2m_e}((4e_{g+})\underline{\nabla}(4e_{g+})^* - (4e_{g+})^*\underline{\nabla}(4e_{g+})) \quad (20)$$

Obviously, this laser induced net ring current has a rather simple structure. Essentially, it consists of two equivalent unidirectional

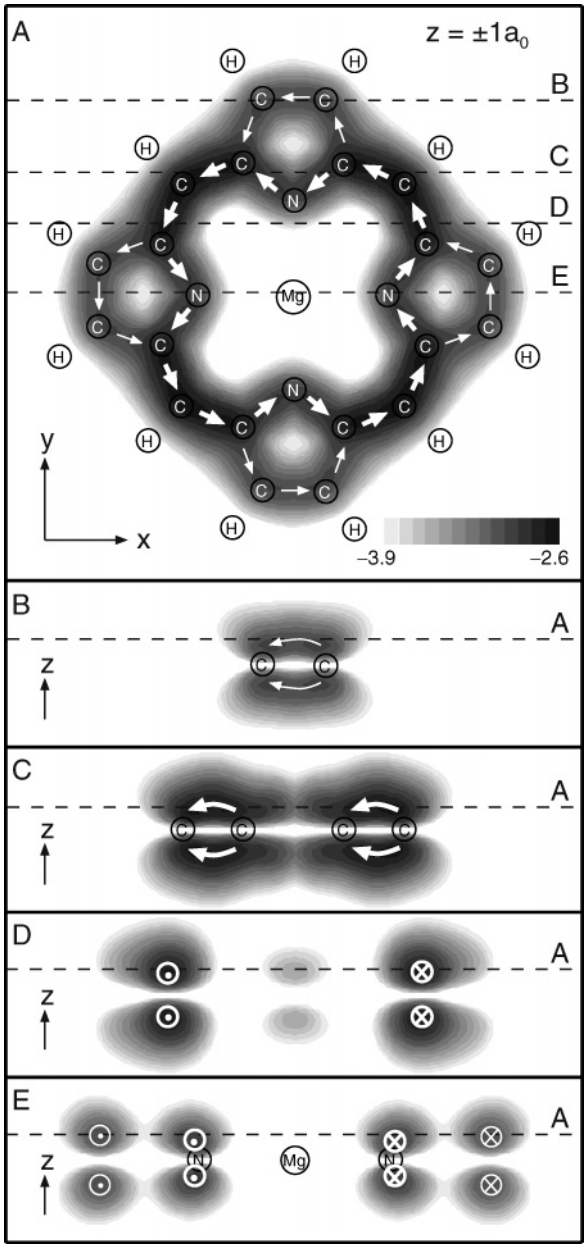

Figure 4. Electronic ring current in oriented Mg−porphyrin induced by the (right) circularly polarized UV π laser pulse (cf. Figures 1 and 2). Panel A shows the flux map for the plane parallel to the molecular *x*/*y*-plane, at a distance $z = \pm 1\ a_0$. Panels B−E show corresponding flux maps for the planes perpendicular to the molecular planes, as indicated by dashed lines B−E in panel A, respectively. Perpendicular cuts of the plane for panel A with those of panels B−E are also indicated by dashed lines marked A in panels B−E. The magnitudes of the fluxes are illustrated in logarithmic scale ($\log_{10}$) by different gray shadings, from the maximum value $\max|\underline{j}(\underline{r})| = 0.0025\ \hbar/(m_e a_0^4)$ to lower ones, in steps of factors of $10^{-0.1} \approx 0.79$.

(right-handed) currents centered in planes parallel to the *x*/*y*-plane at $z \approx \pm 1\ a_0$ and vanishing in the *x*/*y*-plane. These main fluxes branch into strong and weak ones flowing along the inner C−N−C and outer C−C−C−C chains of bonds of the four equivalent pyrrole fragments, respectively, thus forming two parallel main "inner" ring currents around the inner ring of the Mg−porphyrin, accompanied by weak "outer" ring currents. These details depend on the specific electronic excitation. Integrating $\underline{j}(\underline{r})$ over a half-plane yields the electronic current $J = 0.0128\ \hbar/(m_e a_0^2) = 0.528\ \text{fs}^{-1}$ or $I = eJ = 84.5\ \mu\text{A}$, circulating around the principle molecular axis. The corresponding effective current radius, $r = 6.32\ a_0$, is determined by dominant contributions for the domains of the bridges between neighboring pyrrole fragments ($r_{\text{Mg-C}} = 6.45\ a_0$) plus significant ones for the inner ring ($r_{\text{Mg-N}} = 3.88\ a_0$) plus smaller ones for the outer one ($r_{\text{Mg-C}} = 8.10\ a_0$). This electronic current generates a magnetic field, with maximum value $B_z = 0.159$ T at the Mg atom.

4. Conclusion

The quantum simulations presented in Figures 2−4 illustrate ignition of a state-selective valence-type electronic ring current in oriented Mg−porphyrin, excited by an eight-cycle right circularly polarized UV π laser pulse, as designed in sections 2 and 3. It is illuminating to compare these results with the previous approaches which served as motivation for the present development (see the Introduction). This will also allow us to suggest extensions of the present results.

(i) First, it is fascinating to compare the present results for valence-type electronic ring currents generated by means of laser pulses with those induced by permanent magnetic fields. On one hand, the topologies of the flux maps for Mg−porphyrin are similar; that is, they show bifurcated flows with stronger flux along the inner chain of bonds of the ring-shaped molecule, compared to the outer one; compare Figure 4 with Figure 1 of ref 14. This similarity is a consequence of the dominant transitions between similar orbitals involved in the different excitation processes, $(3a_{2u}) \rightarrow (4e_{g+})$,[23] for the laser excited valence-type electronic ring current associated with the selective transition $|1\ ^1A_{1g}\rangle \rightarrow |4\ ^1E_{u+}\rangle$ (compare with alternative patterns for different excitations, see item (v) below!) versus $(1a_{1u})$ and $(4a_{2u}) \rightarrow (4e_{g+})$ for the diamagnetic global ring current induced in Mg−porphyrin by magnetic fields,[14] as derived from the so-called ipsocentric formulation.[13] (Note that, according to ref 23, the highest occupied orbitals, HOMO and HOMO-1, are $(1a_{1u})$ and $(4a_{2u})$, respectively.) Nevertheless, the shapes of the electronic ring currents are not identical; for example, the effective radius of the ring current induced by the laser pulse is $r = 6.32\ a_0$, different from the value $r = 6.85\ a_0$ [16] of the diamagnetic ring current induced by magnetic field.[14] On the other hand, the values of the net electronic ring currents differ by orders of magnitudes, as follows. For the diamagnetic ring current in Mg−porphyrin, Steiner et al. determined the maximum ring current density $j_{\max} = 0.17\ e\hbar/(m_e a_0^4)$ per atomic unit of the magnetic field, $B = \hbar/(ea_0^2) = 235052$ T.[14] This corresponds to the integrated net flux 10.5 nA/T estimated in ref 16. In contrast, the present net valence-type electronic ring current induced by the laser pulse is $I = 84.5\ \mu$A. In other words, a magnetic field of the order of 84500/10.5 T = 8048 T would be required in order to achieve the same net ring current as for the present laser pulse—this request corresponds to more than 100 times the maximum permanent magnetic fields which can be produced with present technology. In conclusion, generation of electronic ring currents by means of circularly polarized laser pulses is much more efficient than the traditional approach based on permanent magnetic fields.

(ii) Second, the present valence-type electronic ring current has been generated by population transfer from the electronic ground state to a single (+) component of an excited degenerate *E* state, specifically, $|4\ ^1E_{u+}\rangle$, with marginal contributions from neighboring states with the same symmetry $|n\ ^1E_{u+}\rangle$. In contrast,

the pioneering approaches of Yeazell and Stroud, Jr.[5,6] prepared atomic Rydberg states circulating along Kepler orbits by means of circularly polarized laser pulses which excite a coherent superposition state, with important contributions from several partial waves with different quantum numbers of orbital angular momentum. By analogy, it should be possible to prepare valence-type electronic wave packets consisting of superpositions of various $|n\ ^1E_{u+}\rangle$ states ($n = 1, 2, 3, 4, 5, 6, ...$) in oriented Mg−porphyrin, for example, by design of corresponding multicolor circularly polarized laser pulses, or by optimal control (see ref 1), or by an impulsive ultrashort circularly polarized pulse with corresponding broad spectral width, that is, shorter than the inverse frequency $2\pi/\omega = 1.21$ fs for the present electron circulation. The latter approach is suggested by translating the lengths and time scales for the scenario of Yeazell and Stroud, Jr.—atomic Rydberg wave packets circulating with diameters of several thousands of bohr radii within milliseconds and typically driven by nanosecond pulses—to the present molecular and femtosecond time domains.

(iii) Third, the method for the present quantum simulations, that is, solution of the time-dependent Schrödinger equation by means of time-dependent expansions in terms of electronic eigenstates and reduction of the expansion to essentially a two-state problem, is entirely equivalent to the technique of Krause et al.[11] The difference is merely in the applications of linearly versus circularly polarized laser pulses to different types of electronic states, yielding ultrafast selective electron transfer[11] versus the present unidirectional valence-type electronic ring current, respectively. Krause et al. also studied effects of increasing intensities yielding multi-photon excitations and, therefore, loss of state-selectivity, suggesting similar effects in our system for future investigation. Another extension is to include competing effects of ionization at higher laser intensities. Gratifyingly, the ionization potential (IP) of Mg−porphyrin is about 6.9 eV,[32] that is, any competing two- or multiple-photon absorption processes would lead, ultimately, to ionization. Extensions of the present approach to simulations of laser driven electron dynamics at moderately larger intensities may, therefore, still be adequate if they aim at comparison with corresponding experimental results for neutral molecules with excitation energies below IP.

(iv) Fourth, previous results for nuclear dynamics driven by circularly polarized IR π laser pulses[17,18] suggest to extend the present quantum simulations from laser driven pure electron dynamics to combined electron plus nuclear dynamics. For example, it will be important to investigate the role of angular momentum. The primary effect of the laser pulse is to excite the electrons, with angular momentum $M_{el} = \langle 4\ ^1E_{u+}|L_{z,el}|4\ ^1E_{u+}\rangle = 2.0\ \hbar$ (or $2.5\ \hbar$) calculated with quantum chemical CIS (or truncated CISD with an active space of 16 electrons in 16 orbitals) approximation. As secondary effect, electron-to-nuclear angular momentum coupling may induce pseudo-rotations of the nuclei (see ref 40), somewhat analogous to rotating molecules in pseudo-rotational cages.[41] The pseudo-rotations are coupled, in turn, to molecular rotations. Analogous excitations of nuclear rotations by electronic currents through helical molecules between electrodes have been discovered recently in ref 42. Since the laser pulse transfers 1 $\hbar$ photonic angular momentum to the molecule, conservation of angular momenta implies that the total nuclear angular momentum is $M_{nu} = 1-2.0 = -1.0\ \hbar$ (CIS). Gratifyingly, these nuclear pseudo-rotations or rotations are rather slow, with periods of the order of one to several hundred fs or ps, respectively. In any case, they take much longer time than the present few cycle laser pulse; that is, the indirect induction of nuclear pseudo-rotations and rotations imposed by conservation of angular momentum is in accord with our assumption of frozen nuclei. Considerations of laser pulses with longer pulse durations would call for combined simulations of electron plus nuclear wave packet dynamics. Applications of the condition 18 for the design of a circularly polarized π laser pulse are, therefore, restricted to pulse durations below ca. 10 fs. Preliminary ab initio molecular dynamics simulations (at CIS level) indicate that for longer pulses, the nuclear wave packet in the excited state may run out of the FC window. To compensate, one may have to apply more complex chirped[43,44] or optimal pulses. Subsequently, the nuclear dynamics in the electronic excited state may induce internal conversion, ultimately to the electronic ground state. Alternatively, the excited state may fluoresce, or spin−orbit coupling may induce intersystem crossing (ISC) to a rather long-lived degenerate triplet state, which may then decay by phosphorescence. Conservation of angular momentum implies that both radiative decays should be special, that is, by spontaneous emission of right circularly polarized light, in the gas phase. In the condensed phase, the excited state may also be quenched by competing intermolecular energy transfer. Efficient ISC to rather long-lived triplet states has been observed in special derivatives of metallo-porphyrins.[45,46] Irrespective of these sequel processes, the present approach calls for ultrashort circularly polarized laser pulses in the time domain below a few fs or even in the as time domain (see refs 2 and 3), with essentially frozen nuclear dynamics.

(v) Fifth, the present mechanism of inducing an electronic ring current by means of a few cycle circularly polarized UV π laser pulse, together with the extensions suggested in items ii−iv, allows the generation of specific electronic ring currents by active laser control. State-selective excitations of specific components of degenerate states carrying handedness as represented by unidirectional electronic ring currents, such as $|n^1E_{u+}\rangle$ versus $|n\ ^1E_{u-}\rangle$, are achieved by means of the circularly polarized laser pulse. For a given, right or left, polarization, this effect is made possible by preorientation of the molecules, implying different transition dipole couplings from the achiral ground state to $|n\ ^1E_{u+}\rangle$ or $|n\ ^1E_{u-}\rangle$. Equivalent applications of the proposed effect should occur in equivalent molecular systems with degenerate states representing opposite handedness, such as $|\Pi_+\rangle$ versus $|\Pi_-\rangle$ states in diatomic molecules. Preorientation may be achieved in environments, such as surfaces or solids, or by means of laser pulses (cf. ref 27). In the latter case, the combined effect of the laser pulses for preorientation and for generation of valence-type electronic ring current may be considered as multi-photon process, similar to preorientation followed by high harmonic generation (HHG) from oriented

(40) Gaus, J.; Kobe, K.; Bonačić-Koutecký, V.; Kühling, H.; Manz, J.; Reischl, B.; Rutz, S.; Schreiber, E.; Wöste, L. *J. Phys. Chem.* **1993**, *97*, 12509.
(41) Manz, J. *J. Am. Chem. Soc.* **1980**, *102*, 1801.
(42) Král, P.; Seideman, T. *J. Chem. Phys.* **2005**, *123*, 184702.
(43) Mishima, K.; Yamashita, K. *J. Chem. Phys.* **1999**, *109*, 1801.
(44) Kallush, S.; Band, Y. B. *Phys. Rev. A* **2000**, *61*, 041401(R).
(45) Wiehe, A.; Stollberg, H.; Runge, S.; Paul, A.; Senge, M. O.; Röder, B. *J. Porphyrins Phthalocyanines* **2001**, *5*, 833.
(46) Freyer, W.; Mueller, S.; Teuchner, K. *J. Photochem. Photobiol. A* **2004**, *163*, 231.

molecules.[47] The present state-selective approach is complementary to traditional induction of electronic ring currents by magnetic fields. The latter are applied, usually, in the domain of linear response; that is, one applies the magnetic field and obtains an electronic ring current with unique shape,[12−16] corresponding to a type of "passive" control; see also the analogous restricted controllability in the domain of linear response to weak field laser pulses.[48] Instead, well-designed intense circularly polarized laser fields may induce ring currents with state-selective target properties—the appearance of two parallel ring currents with branching into main inner and weak outer fluxes around the pyrrole fragments shown in Figure 4 is just one example. It will be a challenge to design laser pulses for alternative patterns, such as switching to strong outer versus weak inner valence-type electronic ring currents or nonstationary electron circulation, and similar applications to other ring-type molecules. These types of specific electronic currents may in turn induce specific magnetic fields, such as in the present case with maximum value $B = 0.159$ T and with characteristic effects on superconducting quantum interference devices (SQUIDs),[50] and on electron and nuclear spins. By extrapolation, the present approach may also serve as a basis for chemical analysis by means of laser pulse excitation combined with nuclear magnetic resonance detection. The maximum value of the magnetic field of an ensemble of molecules may exceed the molecular one slightly, whereas the mean value of B for the ensemble should be smaller than the maximum molecular reference, depending on the density.

An alternative method for monitoring the present electronic ring currents is HHG. Experiments[51] (see also ref 52) and theoretical analyses[53−56] (see also ref 57) for HHG by means of circularly polarized laser pulses exciting ring-shaped molecules from the electronic ground state yield characteristic spectra, for example, specific selection rules which are different from traditional HHG spectra of noncyclic systems (cf. refs 58 and 59). Analogous symmetry selection rules imply characteristic patterns of HHG spectra from symmetric ring-shaped molecules which have been prepared in specific degenerate electronic eigenstates with selected symmetry. These state-selective HHG spectra may serve as an alternative method for monitoring the associated selective valence-type electronic ring currents, such as the present ones in Mg−porphyrin.

Acknowledgment. We would like to express our thanks to Drs. T. Heine (Dresden), K. Heyne (Berlin), S. Macholl (Magdeburg), I. Shenderovich (Berlin), Prof. H.-M. Vieth (Berlin), and Dr. A. Wiehe (Berlin) for advice on electronic ring currents induced by magnetic field and on their detection, and ISC in excited metallo-porphyrins, respectively. Financial support by Deutsche Forschungsgemeinschaft (project Ma 515/23-1) and Fonds der Chemischen Industrie is also gratefully acknowledged.

JA057197L

(47) Itatani, J.; Levesque, J.; Zeidler, D.; Niikura, H.; Pépin, H.; Kieffer, J. C.; Corkum, P. B.; Villeneuve, D. M. *Nature* **2004**, *432*, 867.
(48) Brumer, P.; Shapiro, M. *Chem. Phys.* **1989**, *139*, 221.
(49) Greenberg, Ya. S. *Rev. Mod. Phys.* **1998**, *70*, 175.
(50) Augustine, M. P.; TonThat, D. M.; Clarke, J. *Solid State Nucl Magn. Res.* **1998**, *11*, 139.
(51) Hay, N.; Castillejo, M.; de Nalda, R.; Springate, E.; Mendham, K. J.; Marangos, J. P. *Phys. Rev. A* **2000**, *61*, 053810.
(52) Weihe, F. A.; Dutta, S. K.; Korn, G.; Du, D.; Bucksbaum, P. H.; Shkolnikov, P. L. *Phys. Rev. A* **1995**, *51*, R3433.
(53) Alon, O. E.; Averbukh, V.; Moiseyev, N. *Phys. Rev. Lett.* **1998**, *80*, 3743.
(54) Ceccherini, F.; Bauer, D. *Phys. Rev. A* **2001**, *64*, 033423.
(55) Ceccherini, F.; Bauer, D.; Cornolti, F. *J. Phys. B* **2001**, *34*, 5017.
(56) Baer, R.; Neuhauser, D.; Zdánská, P. R.; Moiseyev, N. *Phys. Rev. A* **2003**, *68*, 043406.
(57) Becker, W.; Lohr, A.; Kleber, M.; Lewenstein, M. *Phys. Rev. A* **1997**, *56*, 645.
(58) Corkum, P. B. *Phys. Rev. Lett.* **1993**, *71*, 1994.
(59) Lagmago Kamta, G.; Bandrauk, A. D. *Phys. Rev. A* **2005**, *71*, 053407.